Warren J. Baker Endowment
for Excellence in Project-Based Learning
Robert D. Koob Endowment *for Student Success*

FINAL REPORT

Final reports will be published on the Cal Poly Digital Commons website (http://digitalcommons.calpoly.edu).

I. Project Title

"Improving Signal Gain for Radio Neutrino Receivers"

II. Project Completion Date

April 13, 2017

III. Student(s), Department(s), and Major(s)

(1) Alexandra Crawford, Physics and Electrical Engineering Depts., Physics

(2)

(3)

IV. Faculty Advisor and Department

Dr. Stephanie Wissel – Physics
Dr. Dean Arakaki – Electrical Engineering

V. Cooperating Industry, Agency, Non-Profit, or University Organization(s)

Jet Propulsion Laboratory (JPL)
EVA Collaboration
Christian Miki
University of Hawaii - Manao

VI. Executive Summary

ABSTRACT

The chargeless, light elementary particles known as neutrinos can be used as probes of extremely energetic and explosive astrophysical objects such as supernovae and quasars. Since neutrinos are extremely rare and difficult to detect, searches for them require large detector volumes to increase the chances of detecting a signal at any one time. By utilizing the transparency of ice to radio waves, the ANtarctic Impulsive Transient Antenna (ANITA) and ExaVolt Antenna (EVA) experiments are designed to monitor over one million cubic kilometers of Antarctic ice at a time, allowing the probability of finding one to ten neutrinos per flight. An increase in detector sensitivity by adding a dielectric lens to the ANITA gain horn antenna aperture [1] and by developing a large reflector antenna within a super-pressure balloon (EVA) is theorized to improve the likelihood of neutrino detection. This paper documents the effects of a dielectric lens on ANITA's signal amplification chain and the characteristics of signal transmission through an EVA prototype antenna.

INTRODUCTION

High Energy (HE) Neutrinos are difficult to detect due to their ability to travel long distances unaffected by interstellar magnetic fields or unabsorbed by other particles. One prevalent neutrino detection method, utilized in ANITA [2] and EVA [3], is to utilize the Askaryan effect to measure their interactions with with dense dielectric materials such as the Antarctic ice. Askaryan emission arises from the interactions of neutrinos with a dense dielectric to produce a secondary shower of particles that emit coherent (in phase) radio waves [2].

ANITA is a high-gain antenna payload (figure 1 right) flown over the Antarctic ice to detect radio signals produced through Askaryan emissions. The commercial antennas on ANITA (developed by Antenna Research Associates) are linearly polarized with two orthogonal feeds and gain from 6-10 dBi over a range of 180 MHz - 1.2 GHz. Each antenna aperture is 1 m^2 with a 22.5^o beam-width. Arranging 16 in a ring allows for a full circular coverage of the ice[2].

EVA is a proposed successor experiment to ANITA that uses a super-pressure balloon to increase the expected flight time by a factor of 3 over ANITA [3]. The design shown in figure 1 (left) also improves on the gain by embedding a reflector antenna inside the balloon with two components: 1. a thin film of aluminum printed on the inside of the balloon and 2. feed antennas suspended in a ring inside the balloon pointing out towards the reflector. One design for the feed antennas under consideration is a compact, deployable, dual-polarized bowtie antenna. Simulations have demonstrated that the reflector antenna system can achieve a gain of over 30 dBi, thereby increasing the sensitivity of EVA over ANITA by a factor of 100 in power [3].

ANITA PROJECT - DIELECTRIC LENS (NOISE FIGURE, POWER, and GAIN)

The goal of the inclusion of the dielectric lens for the wideband ANITA antenna is to improve signal gain as uniformly as possible from 180 MHz to 1.2 GHz while taking into account the increase in noise temperature to the analogue electronics. Based on research from several papers looking into the opacity of different dielectric materials over different frequencies, Polytetrafluoroethylene (PTFE or Teflon) was determined to be the most cost-effective material that works within ANITA's active frequency range. I calculated the noise figure and the output

power for various Teflon lens thicknesses (ranging from 5 to 10 centimeters) based on the rectangular shaped Teflon utilized by Turk et al. The comparison of the gain and noise figure of a lens in the ANITA amplification system was inspired by a 5 dB [5] increase a dielectric had on the gain of a double-ridged wideband gain horn from 1 to 18 GHz.

Using a spreadsheet to list the contributions of all the components of ANITA's amplification system, their noise factor contributions, and the resultant signal power (and voltage), the dielectric contribution was easily added into the system calculations. The noise figure of the lens:

$$NF = 10\log\left(\frac{T}{T_{sys}} + 1\right)$$

is calculated directly from the signal loss experienced within Teflon under the assumption that the entirety of the loss will result in thermal noise. Loss is calculated using the material (Teflon lens) thickness z, the loss tangent of Teflon δ, and a target wavelength λ.

$$Loss(dB) = 10\log\left(e^{-\delta kz}\right)$$

In the loss equation, k is the wavenumber of interest and is inversely proportional to the wavelength. The loss tangent, a fundamental parameter of a material that affects the propagation of EM waves, was observed to not fluctuate significantly at any one temperature over the frequency range for ANITA (180 MHz to 1.2 GHz). Table 1 shows the calculated loss contribution of the Teflon and the resultant signal voltage with the assumption that the dielectric is 5 cm thick and the gain is between 1 dB (minimum contribution) and 5 dB (maximum projected contribution [4]). Changing the material thickness and frequency of interest for the calculations showed that the final voltage across all measured frequencies was not affected by Teflon's noise figure contribution, but from the projected gain the lens provided.

Within the above calculation, the loss associated with the Teflon lens was not a significant contributor to noise in the system compared to the contribution of its gain, so preliminary simulations were made to create a simplified model of the ANITA gain horn and frequency range to study its radiation pattern in detail. The radiation pattern and signal return loss of a simplified ANITA gain horn model as well as the effects of the addition of a dielectric lens were simulated using the High Frequency Structure Simulator (HFSS) by Ansoft. The solid ellipsoidal geometry, inspired by A. Neto et al., was determined to converge incoming planar waves parallel to the optical axis to the far focal point within the ellipse [6]:

$$e = \frac{1}{\sqrt{n}}$$

where the eccentricity of the ellipse (e) is proportional to the index of refraction (n) of the material used. Figure 2 illustrates the ellipsoidal lens used to load both rectangular and square horns in HFSS.

To mimic the broad range of frequencies that ANITA detects, simplified and scaled versions of the ANITA gain horn were constructed and simulated over narrow frequency bands. Scaled structures (both lens and horns) optimized to be solved at 200 MHz, 600 MHz, 800 MHz, and 1200 MHz, were constructed in HFSS and solved. Signal gain measurement results are shown in figures 3-5, comparing the signal gain an elliptical dielectric lens will contribute to a rectangular horn and a square horn, which is closer to the actual ANITA antenna model than a rectangular waveguide. The gain comparison for both the rectangular and square dielectric loaded horns resulted in a discontinuous measurement most likely due to how the program calculates the integration area for this particular model and solution frequency. The rectangular horn gain measurements for the remaining three

solution frequencies (600 MHz, 800 MHz, 1200 MHz) resulted in a closely-matched gain magnitude with the loaded horn model at the solution frequency but diverges as the frequency either increased or decreased. The loaded square horn model's gain results greatly differed from the empty square horn over the entire frequency range. The differences in both results are due to the lack of impedance matching between the dielectric and the horn over the entire frequency range. The general form of the voltage reflection coefficient (Γ):

$$\Gamma = \frac{Z_0 - Z}{Z_0 + Z}$$

for a wave moving from the lens to the horn determines how much of the signal will be reflected from the transition interface. Figure 6 shows shows the magnitude of the impedance measurement comparison between the square horn and the rectangular horn, both with the lens included. Since the dimensions of the lens and horn are optimized for the central or solution frequency for each simulation group, the impedance will not be optimized over all frequencies, which poses a problem for a fixed dielectric lens size over a 1 GHz bandwidth.

The goal of adding a dielectric lens to ANITA was to increase antenna gain for better detection of the faint, broadband impulses from the ice. Even though the noise figure contribution of teflon within the ANITA amplification system is not significant, the impedance mismatch at the dielectric lens to gain horn waveguide interface causes internal reflection within the lens that contributes to signal loss. This is seen as the largest contributor to signal loss over a broadband frequency range because the loss tangent for Teflon over the frequency range of interest remains constant, resulting in a low absorption for the measured frequencies In the configuration considered and the without changing the impedance matching of the antenna, the addition of a dielectric lens within the ANITA gain horns will not contribute to the amplification of the incoming signal.

EVA PROJECT - THEORY, PROTOTYPE, AND MEASUREMENTS

Each dual-polarized bowtie antenna on EVA is designed to detect signal over a large range of frequencies at (ideally) equal sensitivity over the range. Figure 9 shows a simulation of the gain achieved from The EVA antenna system, assuming the feed transmits more than 80% of the total input power over the frequency range 150 MHz to 800 MHz. One of the most important goals during this stage of prototype development is to maximize the amount of signal being transmitted through each port over the entire frequency range 150 MHz to 800 MHz.

The development of the EVA antenna prototype moved from structure design (figure 7 left) to improving the connections from the feeds to the conductive surfaces ("leaves") on each polarization, as shown in figure 8. Testing of the connections moved from using silver solder where the feed intersects the "leaf" to using strips of copper tape with conductive adhesive to avoid stripping the silver printed on the "leaf". The EVA antennas are constructed to have flexible leaves for storage purposes during deployment and expand out to their design shape after launch (figure 7 left) without compromising the integrity of its connections. A highly conductive silver epoxy was used as a permanent connection, shown in figure 8 (right), and a thin plate of aluminum was attached to the underside of the antenna base that acts like a ground plane (figure 7 right). A ground plane ensures that the grounds of the feed are all at tied to the same potential.

To measure the effectiveness and integrity of the "feed-to-leaf" connection, measurements of the impulse reflectivity through a signal port (S-11)

$$S11(dB) = \Gamma_{dB} = 20\log|\Gamma|$$

were taken to find stable results as the connector was moved. The reflection coefficient Γ, is the ratio of reflected to transmitted power. The signal reflectivity per port was converted to a ratio of transmitted (P_{trans}) to total input power (P_o) :

$$P_{total} = \frac{P_{trans}}{P_o} = 1 - \left| 10^{\Gamma_{dB}/20} \right|^2$$

figure 10 illustrates the transmitted signal power ratio over a range of 200 MHz to 800 MHz using different materials to connect the feed to the leaf of an old EVA antenna prototype. A conductive-ink pen, copper tape, and silver epoxy connections were used and compared to the HFSS (High Frequency Structure Simulator by Ansoft) simulation of EVA's transmitted signal per port. The graphs in figure 11 compare only the copper tape and silver epoxy on the new model compared to the HFSS simulation.

The two prototypes, "old" and "new" mentioned in figures 10 and 11, refer to a subtle change in leaf angle and spacing. A change in the shape of the conductive area on the leaf, paired with the position of the connection with the feed, can alter the amount of gain produced at any one frequency. Comparing the radiated power over the entire frequency range for each prototype, the new antenna design and connections have a narrower bandwidth than the older connections. The HFSS simulations on each of the plots in figures 10, 11, 13, and 14 mark the desired minimum 80% transmitted power for the antennas. Looking at figure 11, the range 600 MHz to 700 MHz has an extremely high signal transmission ratio compared to the rest of the frequency range, but the dip in in 200 MHz to 400 MHz is much lower than any point in the distribution of the old prototype (figure 10). The old prototype was much more uniformly transmitting over all frequencies for each connection material. Although the peak transmission ratio has improved between the two prototypes, the narrowing of the frequency range where the signal is transmitted efficiently is problematic.

Looking at the structure of the antenna, metal (measuring tape) is used to support each leaf at 30 degrees. To further improve the ratio of transmitted power through each port, the angle at which the leaf was suspended and the inclusion of metal supports were each investigated. Removing the metal supports to allow for the measurement of several different angles, a single leaf on the antenna was suspended at several different angles to improve the reflection within the port. Figure 12 compares the original power distribution (black) of the leaf compared to the several different angles the leaf was measured at. The improvement of the distribution around 400 MHz led me to question whether exclusion of the metal supports contributed to the improvement since there was little deviation between angles. The results in figure 14 show the inclusion and exclusion of metal supports within the entire structure and the measured leaf have almost no difference as long as sufficient tension is applied to the measured leaf (shown in figure 13). A structure needs to be constructed for the antenna prototype that allows flexibility for deployment and applies a certain amount of tension to each leaf of the deployed antenna.

CONCLUSION

The number of detected neutrinos during any duration of time can be increased by improving the gain of the radio telescopes that look for them. Improving detector gain over a wide range of frequencies for ANITA cannot be achieved by adding a dielectric lens to the amplification system even though the thermal noise (loss) contribution from Teflon is not significant. The impedance mismatch at the dielectric lens and horn waveguide interface over the large

frequency range causes internal reflections that do not contribute to the amplification of the signal. Ensuring that EVA retains a large gain over a wide range of frequencies starts with how efficiently the feeds are transmitting power, which is dependent upon the shape of the leaf, the position of the feed, and the connection material. The application of tension at the end of the leaf improved the transmitted power ratio over the entire frequency range well above the simulated values.

REFERENCES

1. J. P. Thakur, et al. "Large Aperture Low Aberration Aspheric Dielectric Lens Antenna for W-Band Quasi-Optics". Progress in Electromagnetics Research, PEIR 103, 57-65, 2010.
2. P. W. Gorham, et al. "The Antarctic Impulsive Transient Antenna Ultra-High Energy Neutrino detector: Design, performance, and sensitivity for the 2006-2007 balloon flight". Astroparticle Physics, 32, 10-41, 2009.
3. Romero-Wolf, A. "The ExaVolt Antenna Mission Concept and Technology Developments." *Proceedings of the 34th International Cosmic Ray Conference*. 2015.
4. Turk, Ahmet Serdar, and Ahmet Kenan Keskin. "Partially dielectric-loaded ridged horn antenna design for ultrawideband gain and radiation performance enhancement." *IEEE Antennas and Wireless Propagation Letters* 11 (2012): 921-924.
5. Ehrlich, P. "Dielectric properties of teflon from room temperature to 314 C and from frequencies of 102 to 105 c/s." *J. Res. Nat. Bur. Stand* 51 (1953): 185-8.
6. Neto, A., S. Maci, and P. J. I. De Maagt. "Reflections inside an elliptical dielectric lens antenna." *IEE Proceedings-Microwaves, Antennas and Propagation* 145.3 (1998): 243-247.

TABLES

Table 1 : Loss Tangent of PTFE at measured frequency with calculated Loss (dB) and resultant signal voltage (material thickness as 5 cm) at different gain values

Frequency	**Loss tangent [6] (tan δ)**	**Loss (dB)**	**Noise Voltage (mV)** ***No Lens***	**Resultant Voltage (mV)** ***Gain = 1 dB***	**Resultant Voltage (mV)** ***Gain = 5 dB***
180 MHz	2E-4	1.64E-4	35.683	40.036	63.453
550 MHz	2E-4	5.00E-4	35.683	40.036	63.453
1.2 GHz	3E-4	1.64E-3	35.683	40.036	63.453

FIGURES AND GRAPHS

Figure 1 : ANITA antenna telescope (left - photo credit to Christian Miki) and the EVA telescope concept [3] (right)

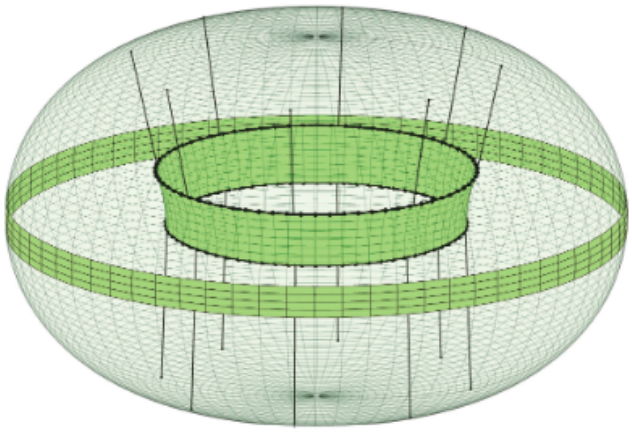

Figure 2 : Ellipsoidal lens within simulations of rectangular (left) and square (right) gain horns

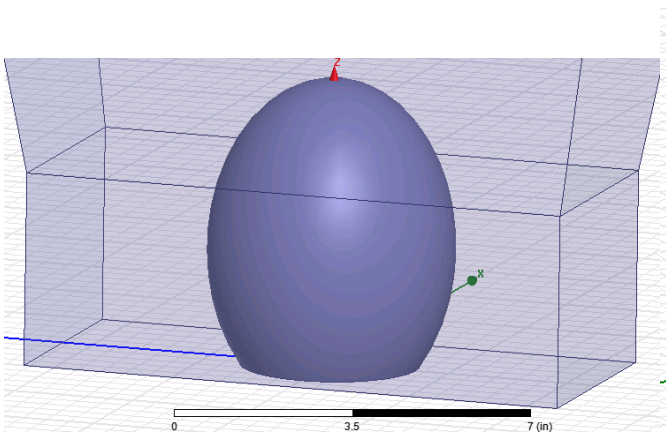

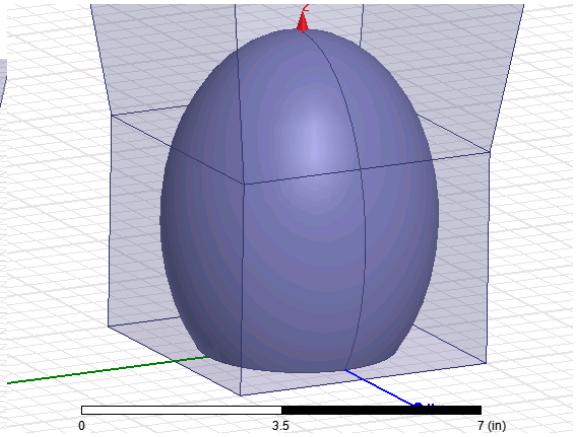

Figure 3 : Gain measurement comparisons (rectangular and square horns) with and without lens at a central frequency of 600 MHz

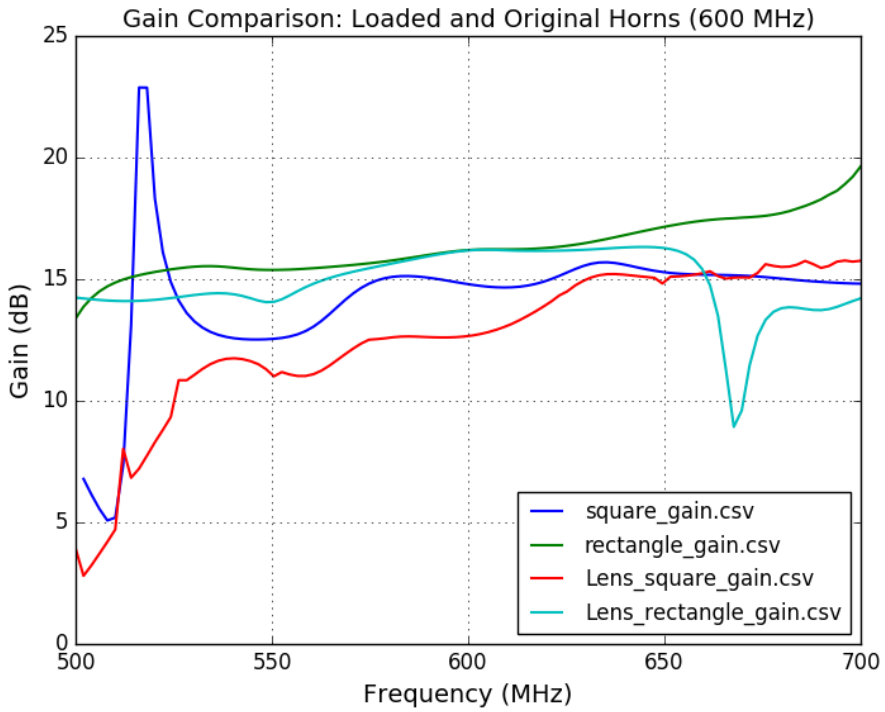

Figure 4 : Gain measurement comparisons (rectangular and square horns) with and without lens at a central frequency of 800 MHz

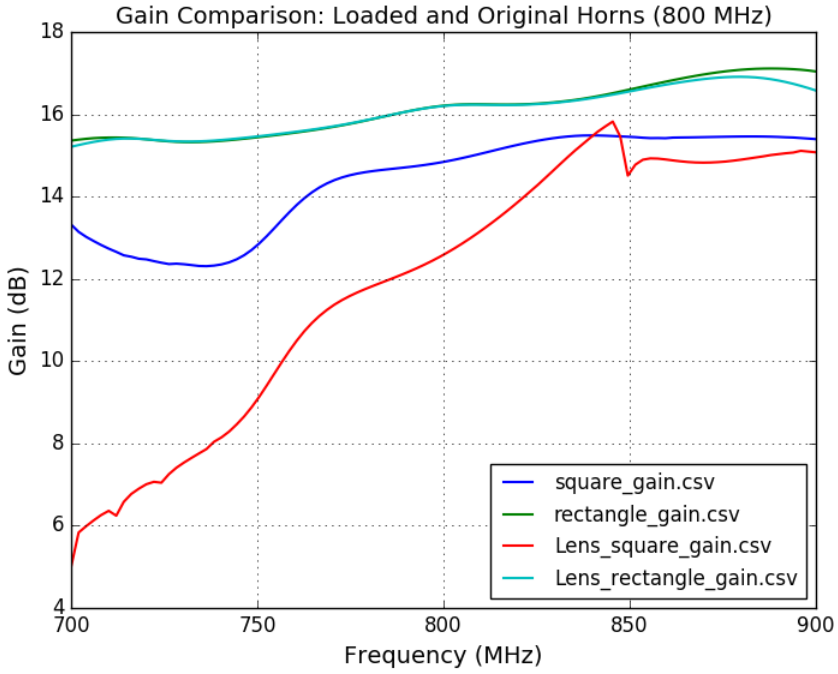

Figure 5 : Gain measurement comparisons (rectangular and square horns) with and without lens at a central frequency of 1200 MHz

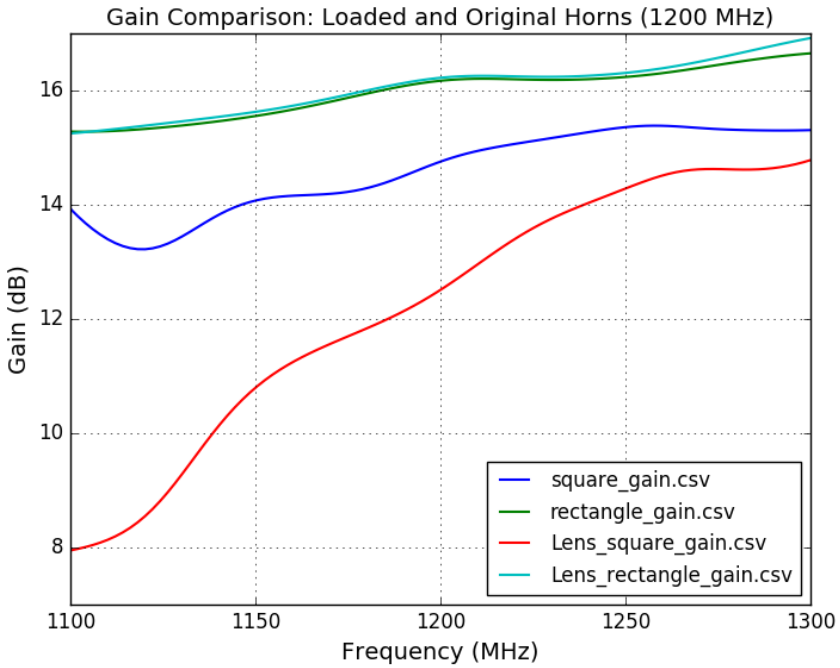

Figure 6 : Impedance match comparison between square and rectangular horns (with lenses) at a central frequency of 800 MHz

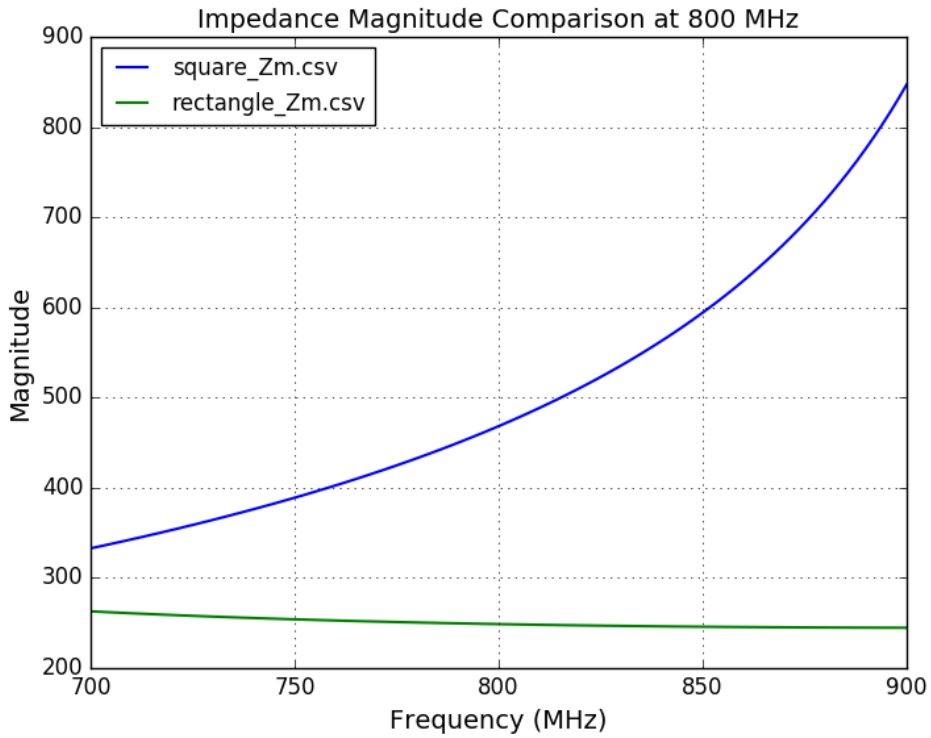

Figure 7 : EVA prototype antenna (left) and aluminum plate addition to ground plane (right)

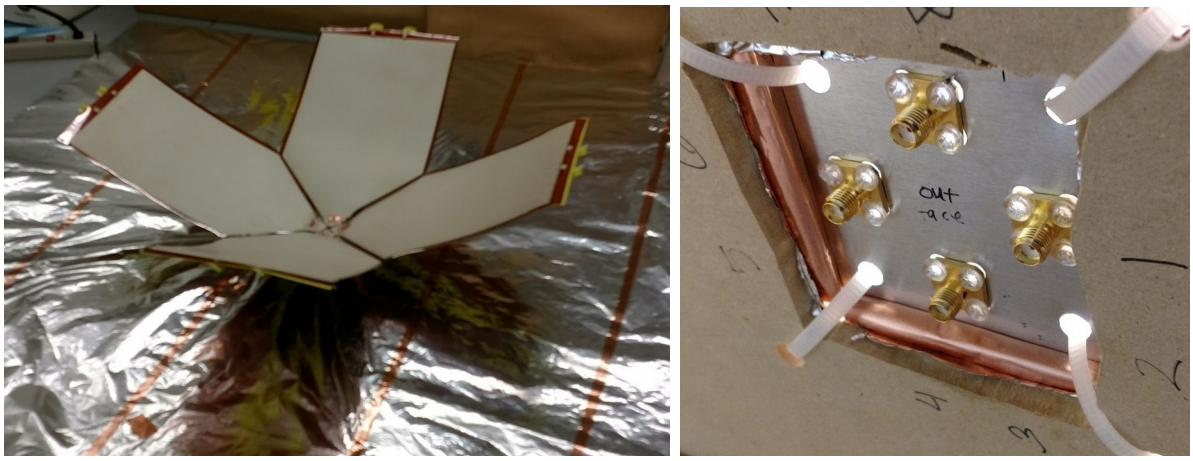

Figure 8 : Copper tape (left) and silver epoxy (right) “feed-to-leaf” connections

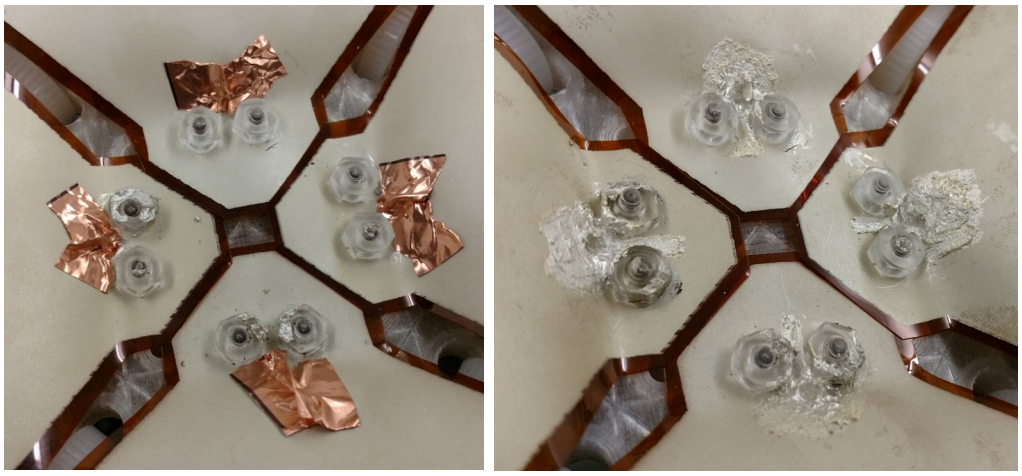

Figure 9 : Simulated gain of EVA antenna system

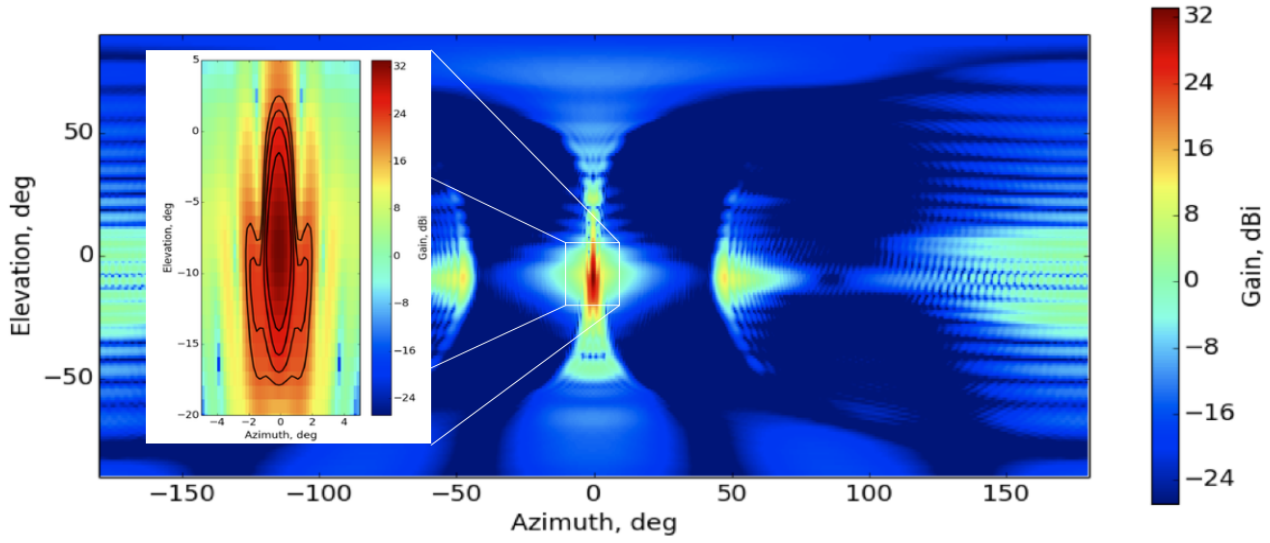

Figure 10 : Comparison of different "feed-to-leaf" connection materials on total power transmitted through signal port for the old prototype (EVA)

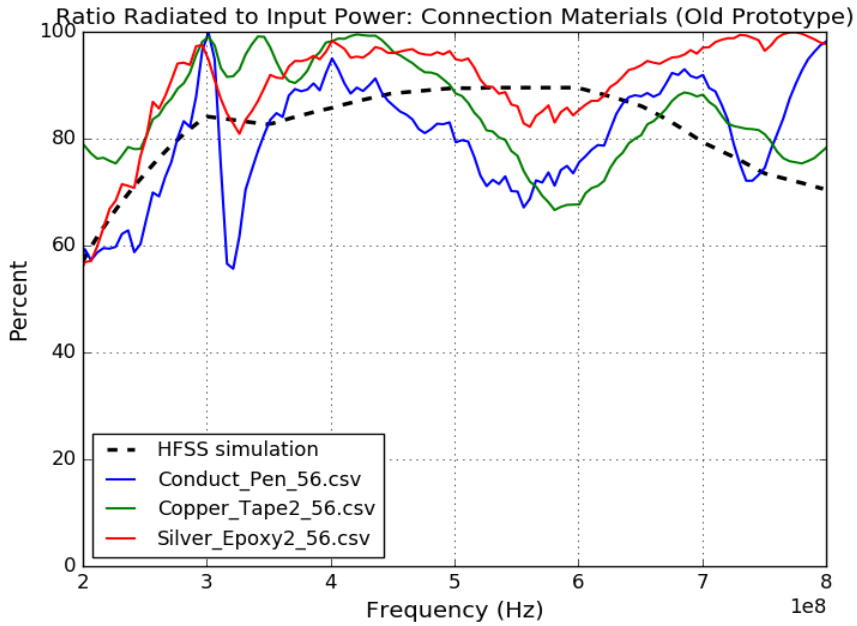

Figure 11 : Measured (vs simulated) total radiated power though each feed (EVA new prototype) comparing silver and copper feed-to-leaf connections

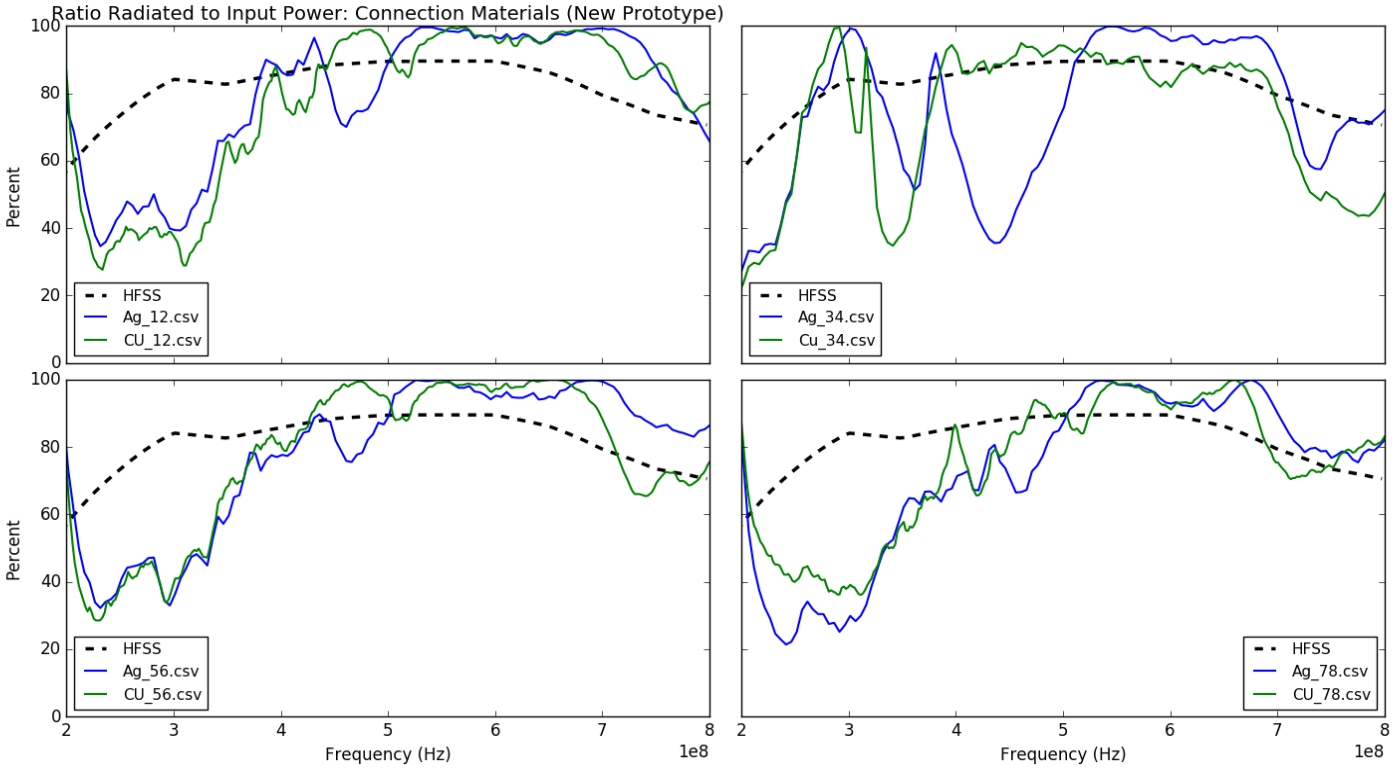

Figure 12 : Total Radiated Power of leaf suspended at different angles without metal supports

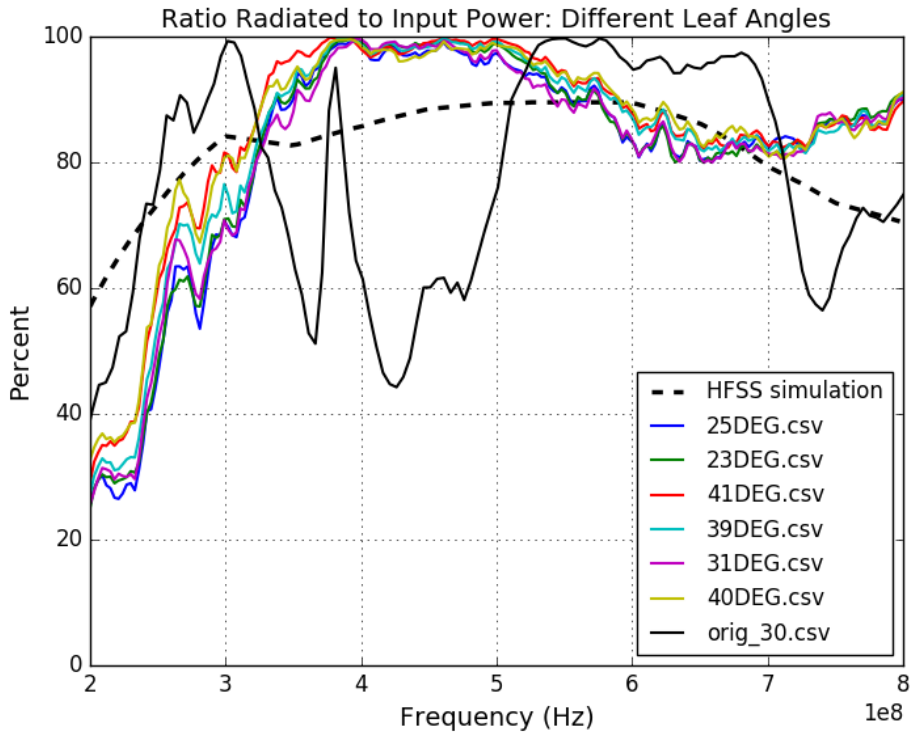

Figure 13 : Application of tension at the end of one "leaf" of EVA antenna prototype

Figure 14 : Improved results in comparison of measured (vs simulated) total radiated power due to application of tension

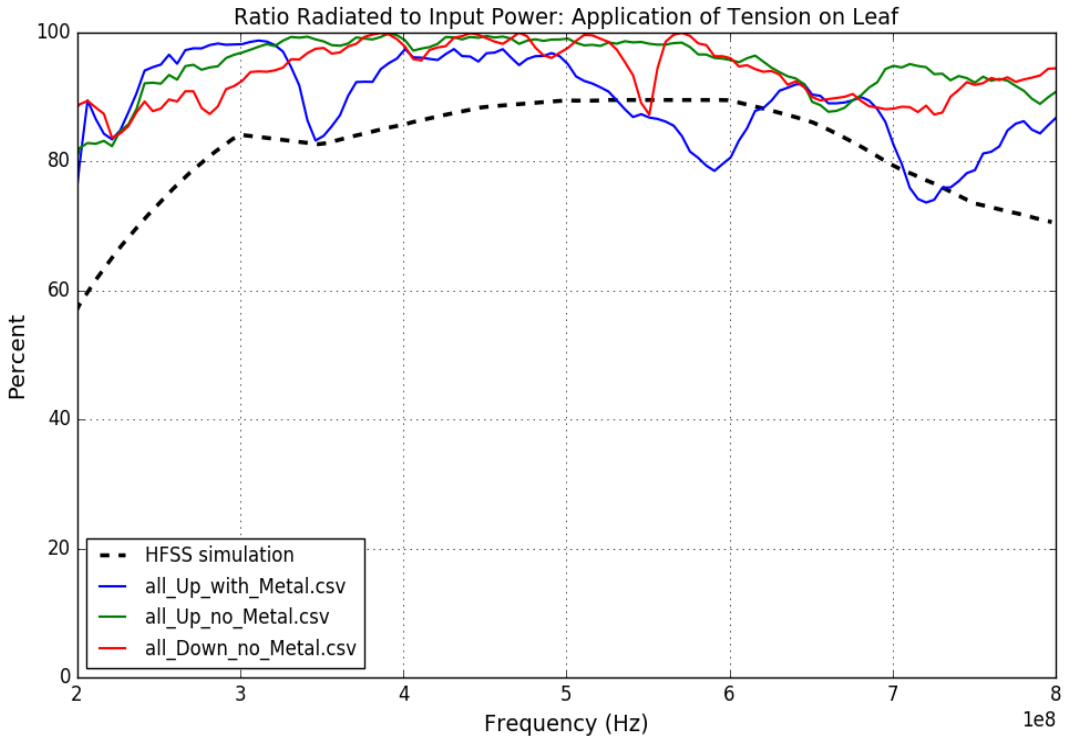

VII. Major Accomplishments

(1) Development of ellipsoidal dielectric lens and determination through simulation in HFSS (High Frequency Structure Simulator by Ansoft) that its inclusion will not improve the signal gain of an ANITA antenna

(2) Improvement above simulated results of total radiated power per signal port of the EVA antenna prototype through physical changes in structure and materials

(3)

VIII. Expenditure of Funds

Date	Vendor	Part Number	Item(s)	Cost	Remaining
11/7/2016	McMaster		Items for prototype construction	$90.71	$2409.29
11/7/2016	RF Depot	24L-NANA-2400S	LMR240 for testing S11s	$422	$1987.29
1/13/2017	McMaster		Items for prototype construction	$177.28	$1810.01
2/12/2017	McMaster		Items for prototype construction	$222.14	$1587.87
			TOTAL SPENT:	**$912.13**	

IX. Impact on Student Learning

In addition to the conclusions I have made in this project, I was able to take away an understanding of how to use specialized pieces of equipment and software as well as a skill of how to manage multiple experiments in tandem. The ANITA project specifically allowed me to spend more than a year learning and utilizing the Ansoft product HFSS (High Frequency Structure Simulator) in a unique application. Many months were spent using trial and error to understand the finer applications of large concepts and theories within HFSS through the different outcomes of several simulations. The EVA project provided the opportunity to use a FieldFox Handheld RF Vector Network Analyzer in the lab as well as refine my skills in Python to handle large data sets. I learned how to calibrate this particular equipment and use it to obtain several different measurements for this application.